Acoustics reveals short-term air temperature fluctuations near Mars' surface

Baptiste Chide[1,*], Tanguy Bertrand[2], Ralph D. Lorenz[3], Asier Munguira[4], Ricardo Hueso[4], Agustin Sánchez-Lavega[4], German Martinez[5,6], Aymeric Spiga[7,8], Xavier Jacob[9], Manuel de la Torre Juarez[10], Mark T. Lemmon[11], Don Banfield[12], Claire E. Newman[13], Naomi Murdoch[14], Alexander Stott[14], Daniel Viúdez-Moreiras[15], Jorge Pla-Garcia[15], Carène Larmat[1], Nina L. Lanza[1], José Antonio Rodríguez-Manfredi[15], Roger C. Wiens[16]

[1]: Space and Planetary Exploration Team, Los Alamos National Laboratory, Los Alamos, New Mexico, USA
[2]: LESIA, Observatoire de Paris, Université PSL, Sorbonne Université, Université de Paris, CNRS, Meudon, France
[3]: Space Exploration Sector, Johns Hopkins Applied Physics Laboratory, Laurel, MD, USA.
[4]: Física Aplicada, Escuela de Ingeniería de Bilbao, UPV/EHU, Bilbao, Spain.
[5]: Lunar and Planetary Institute, Universities Space Research Association, Houston, TX, USA,
[6]: Department of Climate and Space Sciences and Engineering, University of Michigan, Ann Arbor, MI, USA
[7]: Laboratoire de Météorologie Dynamique, Institut Pierre-Simon Laplace (LMD/IPSL), Sorbonne Université, Centre National de la Recherche Scientifique (CNRS), École Polytechnique, École Normale Supérieure (ENS), Paris, France
[8]: Institut Universitaire de France, Paris, France
[9]: Institut de Mécanique des Fluides de Toulouse, Université de Toulouse III Paul Sabatier, INP, CNRS, Toulouse, France
[10]: Jet Propulsion Laboratory, California Institute of Technology, Pasadena, California, USA
[11]: Space Science Institute, Boulder, CO 80301, USA
[12]: NASA Ames Research Center, Mountain View, CA, USA
[13]: Aeolis Research, Chandler, AZ, USA
[14]: Institut Supérieur de l'Aéronautique et de l'Espace (ISAE-SUPAERO), Université de Toulouse, Toulouse, France
[15]: Centro de Astrobiología (INTA-CSIC), Madrid, Spain
[16]: Department of Earth, Atmospheric, and Planetary Sciences, Purdue University, West Lafayette, IN, USA

*Corresponding author: Baptiste Chide (bchide@lanl.gov)

Key Points:

- Sound speed derived temperature is used to study the microscale turbulence at an unprecedented short response time.
- Air temperature experiences fluctuations as high as ±7 K/s, which has never been reported *in situ*, nor resolved by mesoscale atmospheric models
- Sonic temperature fluctuations follow the daytime turbulence pattern and find their origin in complex surface-atmosphere interactions

This is the author manuscript accepted for publication and has undergone full peer review but has not been through the copyediting, typesetting, pagination and proofreading process, which may lead to differences between this version and the Version of Record. Please cite this article as doi: 10.1029/2022GL100333.

Abstract

Acoustics is new on Mars: it allows the characterization of turbulence at smaller scales than previously possible within the lowest part of the Planetary Boundary Layer. Sound speed measurements, by the SuperCam instrument and its microphone onboard the NASA Perseverance rover, allow the retrieval of atmospheric temperatures at 0.77 m above the ground, at 3 Hz, with a ~10 ms response time that is 20 to 100 times shorter than for typical thermocouple sensors used on Mars. Here we report on the first measurements of the sound speed-derived temperature and its fluctuations near the surface. Data highlight large and rapid fluctuations up to ±7 K/s, whose amplitude over such a timescale has never been reported, nor predicted by atmospheric models. These fluctuations follow the daytime pattern of the turbulence and highlight occasional high amplitude events that are likely due to the conjunction of low thermal inertia and strong winds.

Plain Language Summary

The atmospheric surface layer of Mars, is prone to various interactions between the surface and the atmosphere, which control most of the climate and the weather of the red planet. There, large temperature gradients generate an intense turbulence during the daytime. Hence, the measurement of the air temperature variations close to the surface is important to understand the spatial and temporal scales of this turbulence. The SuperCam instrument onboard the NASA Perseverance rover enables the retrieval of the near-surface atmospheric temperatures, and their fluctuations, at an unprecedented short timescale. Sound speed-derived temperatures, also call sonic temperatures, collected over the Northern spring and summer of Martian Year 36 reveal large and rapid thermal fluctuations up to ±7 K/s, whose amplitude over such a timescale is not reported by any weather station sensors, nor predicted by models that simulate small-scale eddies. These fluctuations follow the daytime pattern of the turbulence with a maximum amplitude early afternoon. Some occasional high temperature fluctuation events are observed, suggesting a complex effect of ground properties and local meteorological conditions on the turbulence. Overall, acoustics is a new and promising technique that records a unique view of atmospheric temperature variations near the surface of Mars.

1 Introduction

The Planetary Boundary Layer (PBL) includes the lower atmospheric layers directly in contact with the surface (Petrosyan et al., 2011). On Mars, it plays a critical role, strongly impacting the climate system, as it controls the dust lifting, the volatile fluxes and the exchange of heat and momentum between the surface and the atmosphere (Read et al., 2016; Spiga 2019). Probing the Martian PBL, in particular the near-surface atmospheric temperatures, is of importance to understand the thermal response of the atmosphere to the surface radiative forcing and the spatial and temporal scales of the associated turbulence, indicative of the PBL intensity. Most of the previous landed spacecraft have carried instruments capable of monitoring near-surface temperatures. Standard thermocouples were used on the Viking landers (Hess et al., 1977), Mars Pathfinder (Schofield et al., 1997) and Phoenix (Davy et al., 2010). Curiosity (Gómez-Elvira et al., 2012) and InSight (Banfield et al., 2018) used platinum resistance thermocouples, while thermal infrared spectrometry was used by Spirit and Opportunity (Christensen et al., 2003). These observations, performed at different locations and at sampling frequencies ranging from 0.25 Hz to 2 Hz, provided details of the diurnal and seasonal cycle of atmospheric temperatures, which are mostly dominated by the strong radiative forcing of the surface (Martinez et al, 2017; Banfield et al. 2020). Mars Pathfinder (Schofield et al., 1997), Spirit and Opportunity (Smith et al., 2004) explored the strong daytime thermal gradient, both from the surface up to 1.1 m and from 1.1 m up to 2 km, *i.e.* where the PBL forcing takes place. In particular, Opportunity reported temperature fluctuations as large as 8 K at 1.1 m of height over 40 s (Smith et al., 2006; Spanovich et al., 2006), and these values were used to quantify the intensity of the turbulent activity in the PBL. These large fluctuations are also shown to depend on local ground properties (*e.g.* thermal inertia) and local meteorological conditions such as thermal gradient and dust events (Mason & Smith, 2021).

To further characterize the Martian PBL and the associated turbulence at all scales, additional measurements at higher frequency are needed, typically up to 10 Hz (Petrosyan et al., 2011). The first sound speed measurements on Mars, by SuperCam onboard the Perseverance rover, contributes to filling this gap using sonic thermometry, thus measuring near-surface temperatures through acoustic measurements at a response time of ~10 ms, which is about 20-100 orders of magnitude faster than traditional thermocouples. On Earth, sonic thermometry (based on the dependence of sound speed on temperature) and sonic anemometry (based on the effect of winds on the propagation times of acoustic pulses) are efficient and precise ways to study the microturbulence (Kaimal & Gaynor, 1991), as the response time is limited only by the travel time of a sound wave along its propagation path. Moreover, radiative forcing from direct solar illumination, from which thermocouples suffer, especially on Mars, has no effect on sonic thermometry. Overall, it has been predicted that sonic thermometry on Mars would be a breakthrough to access these unobserved scales (Rafkin & Banfield, 2020).

SuperCam measures the first sound speed at the surface of Mars using its laser combined with its microphone (Maurice et al., 2021). The latter provides the first characterization of the Mars soundscape in the audible range (Maurice et al., 2022). In particular, atmospheric recordings unveil pressure variations down to 1,000 times smaller scales than ever observed before, highlighting the transition to the turbulent dissipative regime where eddy energy is transferred to smaller scales and later dissipated into heat. Active acoustic sensing, relying on the sound source created by the SuperCam laser vaporizing rocks (Chide et al., 2020; 2021), is used to extract sound propagation properties of the atmosphere such as the sound speed and the acoustic attenuation coefficient above 2 kHz. Overall, Mars acoustics is a new effective approach to characterize the high frequency dynamics of Mars' atmosphere.

In this study, we analyze the sound speed measurements on Mars and their associated temporal fluctuations at 3 Hz. These results are compared with the temperatures acquired by the Mars Environmental Dynamics Analyzer (MEDA) at a frequency of up to 2 Hz but with a longer response time (Rodríguez-Manfredi et al., 2021), with the large-scale atmospheric predictions from the Mars Climate Database (MCD) and with the predicted small-scale rapidly-varying PBL turbulence from Large Eddy Simulations (LES) (see Supporting Texts S1-S3 for datasets and models). Our analyses cover the first half of Martian Year 36 (Northern spring and summer), from L_s=5.1°, up to L_s=190°, where L_s is the areocentric solar longitude. This corresponds to the first 378 Sols of the mission (a Sol is a Martian solar day), during the exploration of the crater floor unit of Jezero (Sun et al., this issue). Munguira et al., and de la Torre Juarez et al., (this issue), provide additional analyses of the atmospheric temperatures and their fluctuations as retrieved by MEDA during the same period. We introduce the sonic thermometry method (Section 2), then present three results: the sonic temperatures (Section 3.1), their associated rapid fluctuations (Section 3.2), and their diurnal and seasonal evolutions (Section 3.3).

2 Methods: first use of the sonic thermometry on Mars

The recording of SuperCam laser-induced acoustic signals provides a unique opportunity to measure directly and repetitively the local sound speed, using the propagation time of the laser-induced acoustic wave as it travels from the ground up to the microphone, on top of Perseverance (Fig. 1). Given the strong vertical temperature gradient in the atmosphere during the daytime (up to 35 K/m, Rodríguez-Manfredi et al., 2022), the sound speed decreases along the acoustic propagation path. Considering a bulk approximation of the temperature evolution with height using a log-profile within the surface layer (Fig. 1a), the sound speed measured corresponds to a height of 0.77 m above the ground (see Supporting Text S4). Across all observations, the measured sound speed ranges from 244 m/s (Sol 365 at 8:49 Local True Solar Time, LTST) to 270 m/s (Sol 357 at 12:47 LTST). Each sound speed measurement is then converted into air temperature, hereafter called "sonic temperature", considering the ideal gas law, correcting the specific heat at constant volume for the unique sound speed dispersion observed on Mars (Maurice et al., 2022) due to CO_2 at low pressure (see Supporting Text S5).

Furthermore, as the acoustic wave propagates in a moving medium, the measured sound speed is influenced by the background wind velocity (*e.g.* rapid gusts and vertical drafts), projected along the propagation path. MEDA wind data (velocity and direction), when collected simultaneously, are used to correct the measured sound speed. However, winds measured by the MEDA wind sensors may divert from the winds cumulated along the acoustic path: first, Perseverance itself induces perturbations of the wind flow in its vicinity as compared to the acoustic path. Second, turbulent winds are eddies embedded in a background flow, and the microphone is sampling them over a very short timescale, at frequencies that MEDA is averaging over, so the microphone is resolving those eddies (Stott et al., this issue). Therefore, the wind measured by MEDA may not be an accurate indicator of the short period horizontal winds experienced along the acoustic path. Hence, the corrected sound speed includes the contribution for the atmospheric temperature, vertical up/downdrafts not retrieved by MEDA and possible unresolved turbulent gusts. Furthermore, one must consider that while the acoustic measurement is quasi-instantaneous, it is integrated along the propagation path of several meters, and thus any sound speed fluctuations on length scales smaller than that are not resolved. For typical wind speeds of 5-10 m/s (Viúdez-Moreiras et al., this issue) and typical propagation paths of 2-5 m the volume of atmosphere that is being sampled by the acoustic pulse is exchanged on timescales of 0.2-1 s.

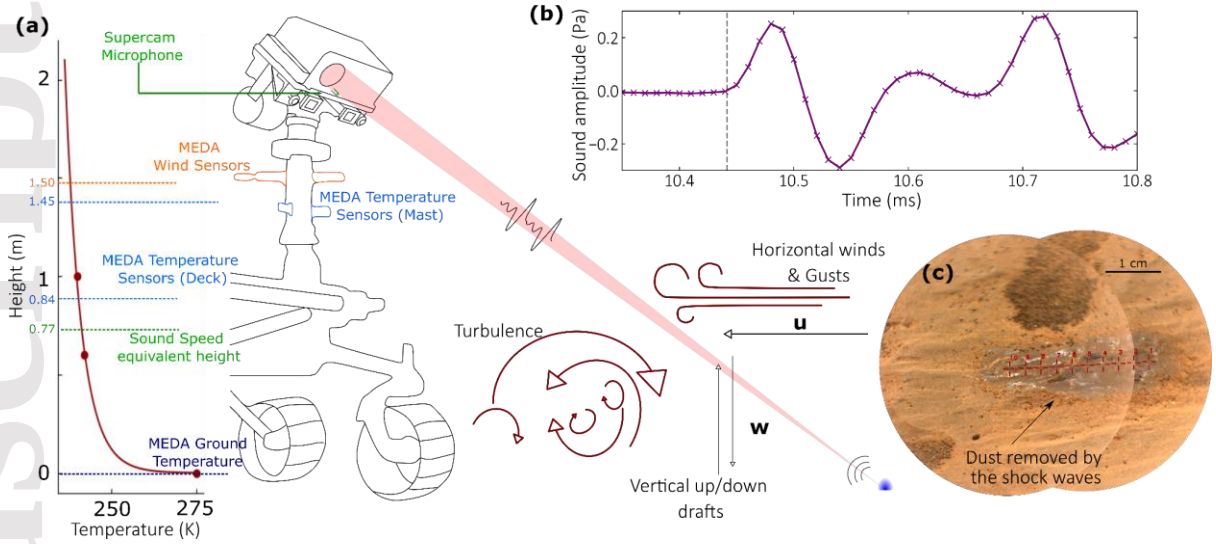

Figure 1. (a) Schematic of the experiment and various sensors. The temperature profile (L_s=100°, 14:00 LTST) is extracted from the MCD and interpolated with a log-profile. (b) Acoustic signal showing the laser-induced direct arrival and its echo on the rover head (Chide et al., 2019). The arrival time is shown by the gray dashed line. (c) Context image of a SuperCam raster on target Tely (Sol 362, 10 points, 30 laser shots each). Laser-induced pits are visible; dust is removed by the shock-waves.

3 Results

3.1 The sonic temperature of Mars.

The daytime evolution of sonic temperatures (Fig. 2a) follows the diurnal cycle observed by MEDA at 0.84 m: increasing during the morning, reaching a maximum around 13:00 to 14:00 LTST and then decreasing until dusk (Munguira et al., this issue). Over the first 378 Sols of the mission, the sonic temperature at 13:00 LTST (Fig. 2b) slightly decreases up to around aphelion (L_s=75°), then increases during the Northern summer up to the equinox (L_s=180°).

These values are compared with MCD simulations at 0.77 m over the same period (see Supporting Text S3). In general, both sonic and MEDA temperatures agree with MCD predictions, but MEDA data peak earlier in the day. This difference could be due to local changes in surface properties (*e.g.* thermal inertia) compared to what is set in the MCD (in which surface properties and environmental diagnostics are averaged over the ~200 km grid scale) or to the interpolation scheme for the temperature profile in the near-surface layer in the MCD, which is not tuned to match observations and which doesn't include all subgrid-scale effects and perturbations. The agreement with both warm and climatology scenarii is excellent up to L_s=140°. Thereafter, the *in situ* data match better with the warm scenario (Fig. 2a) which is concomitant with the increase of dust seen at Jezero (Lemmon et al., this issue), making this season warmer than the multi-year averaged prediction. In fact, daytime atmospheric temperatures after L_s=130° remain even higher than the MCD predictions for the warm scenario, highlighting the strong impact of local dust lifting events occurring in Jezero on the near-surface temperatures (Newman et al., 2022). The agreement with the warm scenario might also be reinforced by the change of albedo, and not exclusively the opacity (see Munguira et al., (this issue) for the albedo influence on temperatures).

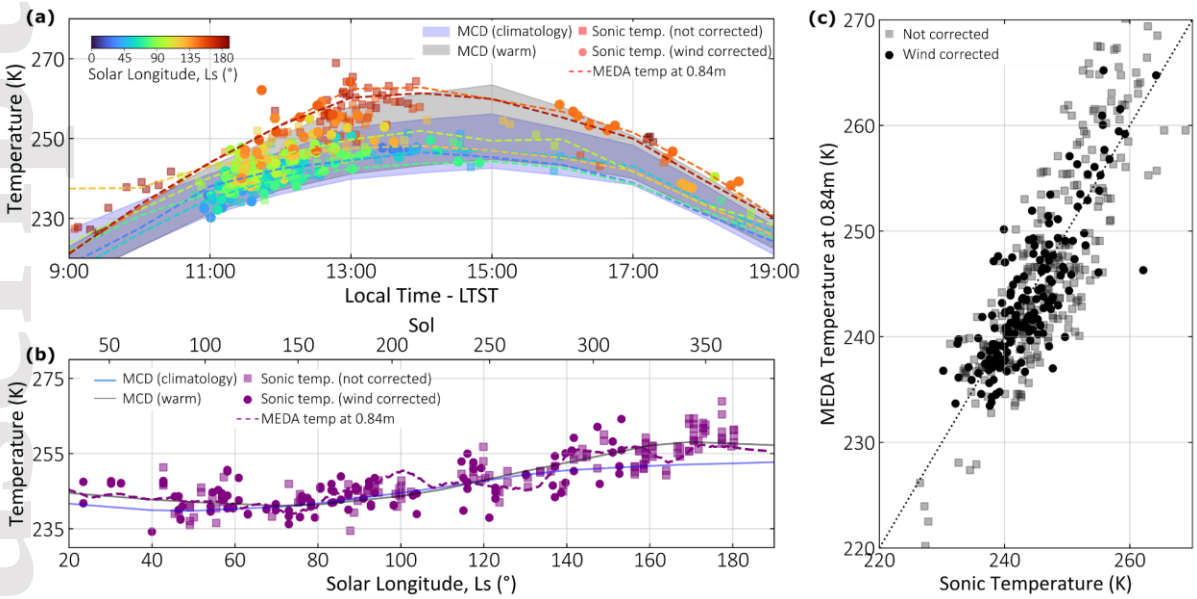

Figure 2. (a) Sonic temperature daytime evolution (circles and squares) compared with 30-sol averaged MEDA temperature at 0.84 m (dashed lines) and with MCD predictions at 0.77 m (shaded): hourly extremal values over L_s=0°-190° for the climatology (blue contour) and warm scenario (gray contour). (b) Sonic temperature seasonal evolution between 11:00 and 14:00 LTST (purple points), compared with MEDA temperature evolution at 0.84 m and 13:00 LTST (purple dashed line). Blue and gray lines represent MCD simulations at 13:00 LTST, for both scenarii. (c) Correlation between sonic temperatures and MEDA temperatures at 0.84 m. For each panel, circles represent wind corrected acoustic data, and squares when wind data were not available.

Fig. 2c shows the one-to-one correlation between sonic temperatures and MEDA temperatures at 0.84 m. Wind corrected values yield a ±2.4 K median absolute difference with MEDA, whereas the difference between MEDA and non-corrected values is ±3.6 K. Hence, the wind correction improves the restitution of the sonic temperatures. However, even without wind data, acoustics provides an efficient measure of air temperature. In addition, microphone data are statistically 0.6 K higher than MEDA's, which is consistent with the sonic temperature height being below MEDA at 0.84 m. This bias confirms that the 0.77 m equivalent height for sonic temperature is reliable, which validates the log-profile considered for the temperature (see Supporting Text S7 and Fig. S2).

Overall, acoustics gives access to the diurnal and seasonal changes of the near surface temperature with a precision comparable to traditional thermocouple-based sensors.

3.2 Evidence of large and rapid near-surface temperature fluctuations.

One of the strengths of the laser-microphone combination is its fast response time, allowing the retrieval of each sonic temperature in ~8 ms for targets at 2 m, up to ~24 ms at 6 m, timescales that are 20 to 100 times shorter than the usual 0.5-1 s response time of weather-station sensors on Mars (Munguira et al., this issue). The sample acquisition induced by the laser repetition rate is 3 Hz, compared to 0.5-2 Hz for temperature sensors.

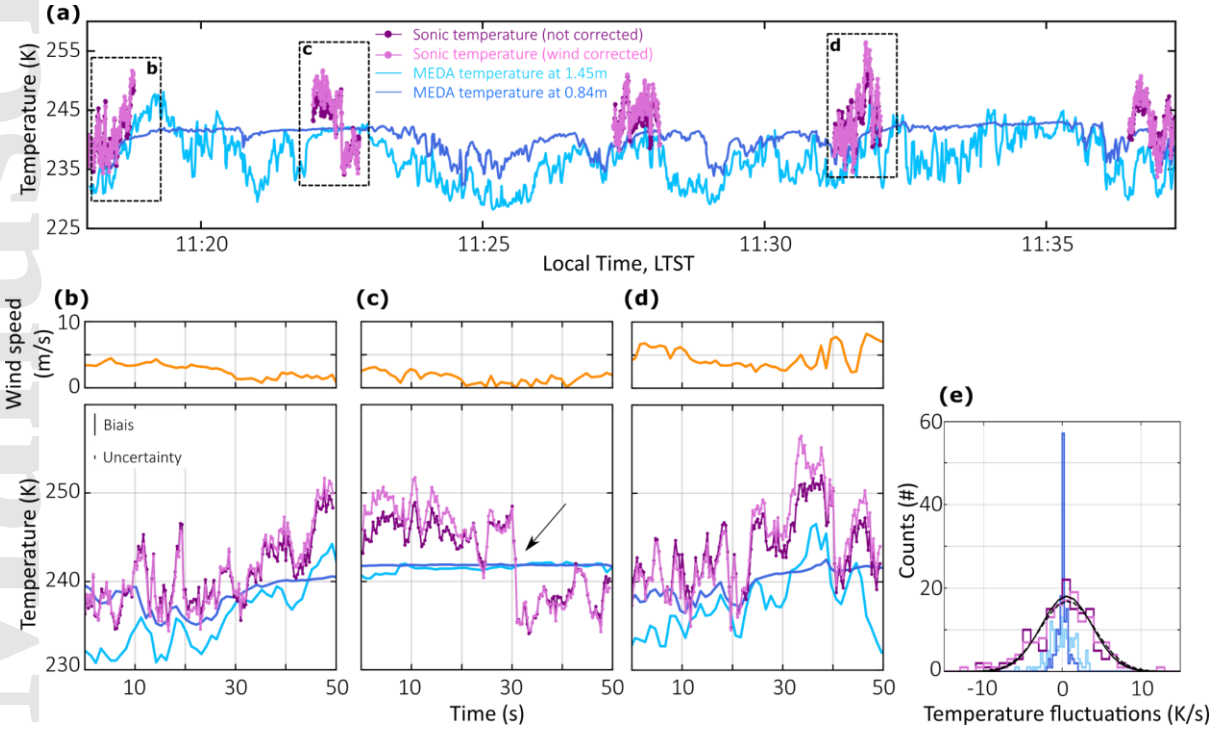

Figure 3. (a) Evolution of the sonic temperature for target Villette (Sol 189, 5 points of 150 laser shots each), compared with MEDA temperatures at 1.45 m and 0.84 m. (b-d) Close-up views of the three 50 s long bursts indicated in (a) and compared with MEDA temperature and wind measurements. The top left vertical bars indicate the error budget: the bias corresponds to the error on the distance, the uncertainty corresponds to the uncertainty on the propagation time (see Supporting Texts S4, S5). The arrow in panel (c) indicates the temperature drop discussed in the main text. (e) Histogram of the time derivative temperature over the data displayed in panel d. Microphone data (both wind corrected in pink and not in purple) are fitted with a Gaussian distribution, in solid and dotted lines respectively.

Fig. 3 highlights the short timescale variations of the sonic temperature measured for a SuperCam target and compares with simultaneous MEDA temperature and wind measurements. Fig. 3a and close-up views in Figs. 3b-d show some clear correlations between the sonic and MEDA temperature fluctuations, even over 5 s. The sonic temperature follows the trend observed by MEDA at 1.45 m of height, whereas MEDA temperatures at 0.84 m record smoother fluctuations (Fig. 3c), most probably because of the sheltering from the wind of these sensors by the rover itself (see Supporting Text S2). In contrast, the acoustic method samples open air away from the rover. Moreover, for every microphone recording, the sonic temperature integrates a quasi-frozen state of warm and cold eddies across the acoustic pathway, whereas MEDA in general measures the temperatures of different eddies that are being carried by the local wind to the sensor.

The most striking observations are the rapid and large amplitude variations recorded by acoustics that are not seen in MEDA data. Sonic temperatures vary by ±4 K/s on average (Fig. 3e), whereas MEDA averaged values range from ±0.5 K/s to ±2 K/s at 0.84 m and 1.45 m of height respectively (see Supporting Text S6). Hence, the microphone sheds light on a much faster turbulence regime than MEDA can observe.

The larger variability observed in acoustic data may also imply a significant contribution from turbulent (high-frequency) winds. Although these results suggest that the wind correction does not change substantially the distribution of the sonic temperature fluctuations (Fig. 3e), winds measured by MEDA only correct for a low frequency component. Rapid gusts and/or vertical drafts are not corrected from the measured sound speed and may contribute to the small-scale variability of the acoustic data. Especially, one question is whether the sudden drop in the sonic temperature of -13 K in 1 s seen in Fig. 3c, could be entirely related to a wind perturbation instead of an actual atmospheric cooling. This drop, and its associated perturbation lasting for at least 20 s could correspond to a rapid downdraft of 5.2 m/s (it is unlikely at 0.77 m above the surface and it would also locally induce adiabatic warming), or a 12 m/s horizontal gust (which might be missed by MEDA due to geometric effects), or a mix of both. In summary, sonic temperatures yield new observations of short timescale thermal fluctuations in the Martian PBL. Therefore, sonic temperature fluctuations are a novel way to explore the microscale turbulence of the PBL and study it as a function of the local time and season.

3.3. Diurnal and seasonal evolution of the temperature fluctuations.

The sonic temperature fluctuations are represented as a function of local time (Fig. 4a) and season (Fig. 4b). Average fluctuations range from 1 K/s to 7 K/s, which are consistent with the magnitude of variations observed by Spirit and Opportunity over longer timescales (Mason & Smith, 2021). For the earliest measurement available in the morning, fluctuations range around 2.5-3 K/s. They increase throughout the morning to reach bulk value of ~3-5 K/s and up to 7 K/s between 12:00 and 14:00 LTST . In the afternoon, the fluctuations decrease, and after 17:00 LTST the observed fluctuations are ~1 K/s due to the collapse of the boundary layer, and the vanishing of the near-surface thermal gradient. Daytime variations are consistent with the development of the atmospheric turbulence. To illustrate this, Fig 4a shows the maximum temperature deviation (T-T_{mean}) as obtained over time in the LES across the simulated domain. Although these modeled temperature deviations are not quantitatively comparable to the observed fluctuations as the LES only resolves the largest eddies and not scales as small as those probed by the microphone, they remain a good proxy of typical turbulent fluctuations. Maximum temperature deviation in the LES is obtained between 12:00-14:00 LTST, as for the sonic fluctuations. The fact that the temperature fluctuations in K/s in the LES are lower than observed in the acoustic data highlights that what the microphone sees is probably linked to small-scale eddies (see Supporting Text S3).

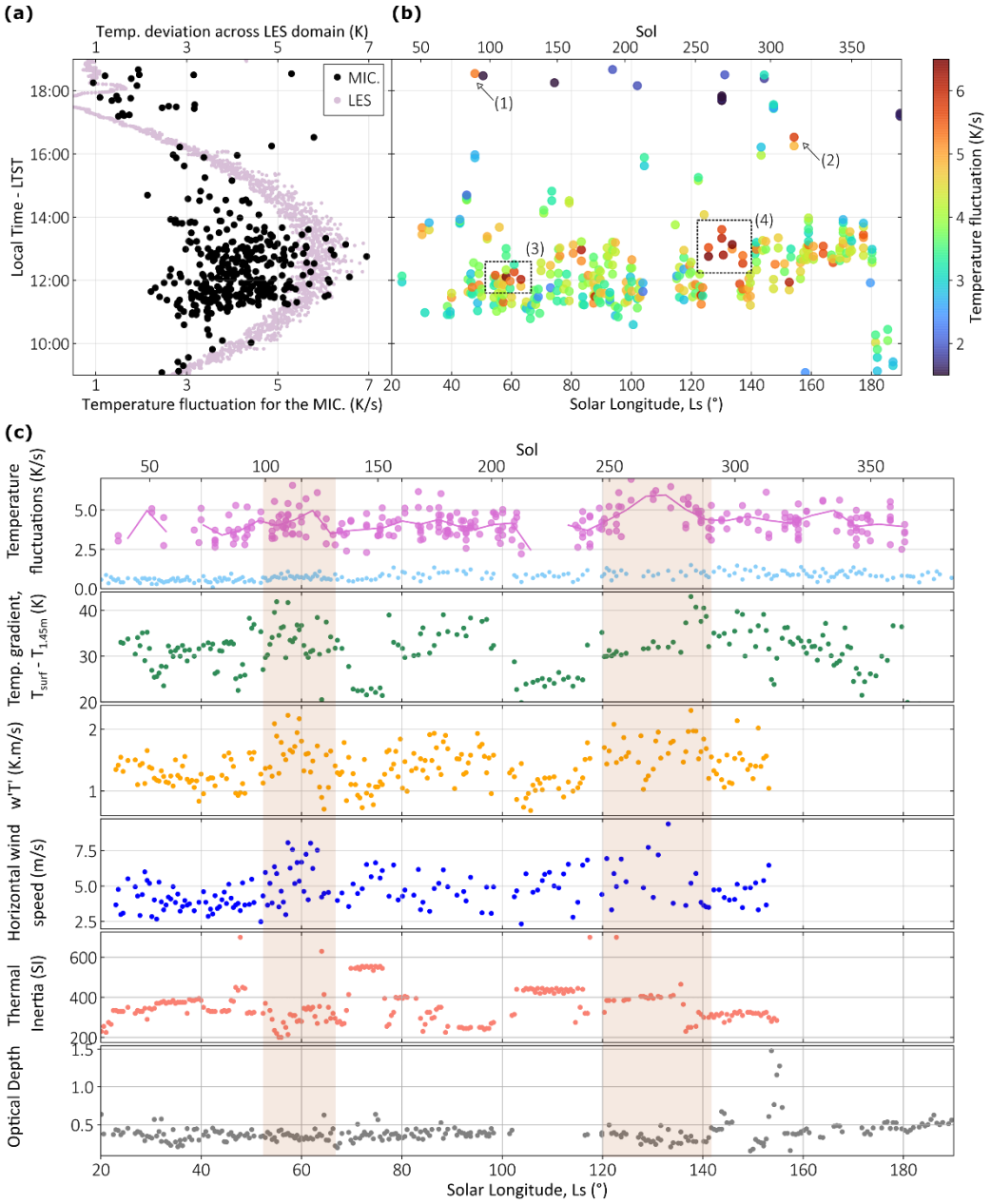

Figure 4. (a) Diurnal evolution of the sonic temperature fluctuations (black), compared with the temperature deviation across the LES domain (pink, see text). (b) Temperature fluctuations as a function of local time and solar longitude. Annotations indicate singular large temperature fluctuation events discussed in the text. (c) Seasonal evolution of the sonic temperature fluctuations compared with other meteorological and ground conditions: sonic temperature fluctuations (pink points) between 11:00 and 14:00 LTST. The solid pink line represents the mean over 8 sols. It is compared with temperature fluctuations recorded by MEDA at 1.45 m (light blue points). In green, the difference between the ground and the atmospheric temperature at 1.45 m; in yellow the covariance between vertical wind and air temperature *w'T'*; in blue horizontal wind speed; in orange thermal inertia; in grey the atmospheric column optical depth. For the thermal gradient, *w'T'* and horizontal wind, value are acquired at the average LTST of the acoustic acquisitions for each sol. The orange boxes highlight the events (3) and (4) observed in Fig. 4b.

Sonic temperature fluctuations do not show any apparent seasonal trend (Fig. 4b), which seems consistent with Opportunity's observations (Mason & Smith, 2021). Nevertheless, this will be investigated further over a full Martian year, in a future work. However, specific high fluctuation events are observed, for instance 5.3 K/s after 18:00 LTST on Sol 89 (annotation 1 Fig. 4b, L_s=48°). Considering the mean north-easterly wind measured by MEDA at this local time, and the position of the target with regard to the rover orientation, it is likely that these fluctuations are due to turbulence-induced by warm air plumes heated by the rover's radioisotope thermal generator, and carried across the acoustic path by local winds (see Supporting Fig. S3). On Sol 315 at 16:25 LTST (annotation 2 Fig. 4b, L_s=154°), two large fluctuations of 4.8 K/s and 5.8 K/s are observed. Such values are significantly higher than the mean of other sonic measurements around this local time. This event could correspond to an increased turbulence due to the regional dust storm observed at Jezero between Sols 313 and 318; turbulence reinforcement in a dustier context is predicted by LES accounting for dust transport, *e.g.* Wu et al., (2021). This event also matches with the timing of an excess grain motion between two consecutive SuperCam images of this target, confirming the strong atmospheric activity at this time (Lemmon et al., this issue). Therefore, microphone data could have caught shear-driven gusts, as already observed on Mars by InSight (Chatain et al., 2021).

Two other sets of high temperature fluctuation events, each spanning ~10 Sols (annotations 3,4 Fig. 4b) are noticed around L_s=62° and L_s=130°. To interpret these events, they are compared with other local and meteorological conditions acquired at the same time by MEDA (Fig. 4c). During the first 378 Sols, the rover drove for about 5.1 km over various terrains, which implies changes of thermal inertia over time. Other parameters, such as surface albedo, local surface roughness and topography vary too (not shown), which affects the local turbulence and thus complicates the interpretation of these events. However, we observe that the temperature gradient (defined as T_{surf}-$T_{1.45\,m}$) is strongly linked with the thermal inertia: when the thermal inertia is minimum (*e.g.* at L_s=55°, L_s=90° and L_s=140°), the daytime thermal gradient is maximum and conditions are more unstable. The event observed in acoustic data at L_s=62° compares well with a high thermal gradient and is also consistent with stronger horizontal winds and a high value of the covariance between vertical wind and air temperature, also called $w'T'$ (derived for the first time on Mars from MEDA measurements by dividing the sensible heat flux by the air density and the specific heat of CO_2, see Martínez et al., (this issue)). The second event (L_s=130°) is more difficult to interpret with thermal inertia and temperature gradient. However this increase of the sonic temperature fluctuations is still consistent with high values of $w'T'$ and horizontal winds. As inferred by Mason & Smith, (2021) and as shown here, dust optical depth has a negligible impact on the amplitude fluctuations. Consequently, the high fluctuations observed on Sol 315 (annotation 2, Fig. 4b), during the dust storm, are likely the result of large-scale dynamics rather than a dustier atmosphere. Finally, Fig. 4c shows a good correlation between sonic temperature fluctuations and $w'T'$. Indeed, as described in Section 2, the sonic temperature takes into account variations in air temperature and vertical wind speed, the same parameters involved in $w'T'$. It strongly confirms the consistency of these two datasets, which are obtained from two independent instruments and methods.

4 Conclusion and Perspectives

In conclusion, the sound speed-derived air temperature, called sonic temperature, is measured using the laser-microphone combination of SuperCam, with a fast response time, 20 to 100 times shorter than typical temperature sensors used on Mars. The sonic temperature follows the diurnal and seasonal evolution of the temperature recorded by MEDA and predicted by a global climate model, MCD. Hence, it demonstrates the ability of this new acoustic method to measure near-surface temperatures on Mars with a precision comparable to thermocouple-based sensors like MEDA. More importantly, owing to the short response time of this new measurement, we identify temperature fluctuations up to ± 7 K/s near the surface, which

is not reported over this short timescale by current weather sensors on Mars. Indeed, the microphone captures small-scale eddies that are not resolved by mesoscale LES models either. The diurnal evolution of these fluctuations follows the development of the atmospheric turbulence. Occasionally, high temperature fluctuations are observed, that are likely associated with a dust storm-induced turbulence or shear-driven gusts, or due to complex interactions between surface (*e.g.* thermal inertia) and atmospheric properties (*e.g.* strong winds, vertical drafts).

Going further, our current dataset is mostly limited between 11:00 and 14:00 LTST, and it has a low sampling coverage compared to MEDA, which performs quasi-continuous observations. A larger time coverage is needed, and is currently being acquired by Perseverance, especially to study the nighttime turbulence (Chatain et al., 2021; Pla-Garcia et al., this issue). In future studies, sonic temperature measurements will also be combined with the high frequency pressure fluctuations captured during microphone recordings (Stott et al., this issue) to explore the turbulence diurnal cycle with two different metrics. In addition, the small-scale large-amplitude fluctuations reported here remain to be simulated by numerical models resolving small-scale eddies, which have seldom been explored for Mars. For instance, these observations open the door to new turbulence models that would couple LES outputs with direct numerical simulations (DNS) to resolve such fine-scales (Bury et al., 2019). Finally, our results call for a new generation of instruments, relying on acoustics, to shed light on this high frequency regime of the Mars atmosphere (Banfield et al., 2016). Such a fine-scale characterization of the local turbulence combining high-frequency models and *in situ* observations will be critical to fully understand the turbulence.

Acknowledgments

The authors thank the Mars2020 Science and Engineering teams for their work supporting the mission that has enabled the scientific research presented in this manuscript. Several contributors are supported by CNES for their work with SuperCam on Perseverance (Mars 2020). B.C is supported by the Director's Postdoctoral Fellowship from the Los Alamos National Laboratory.

Open Research

All Perseverance data used in this study are publicly available via the Planetary Data System:

- SuperCam: Wiens, Roger C.; Maurice, Sylvestre (2021). Mars 2020 Perseverance Rover SuperCam Raw, Calibrated, and Derived Data Products. PDS Geosciences Node. https://doi.org/10.17189/1522646
- MEDA: Rodriguez-Manfredi, Jose A; de la Torre Juarez, Manuel (2021). Mars 2020 Perseverance Rover Mars Environmental Dynamics Analyzer (MEDA) Experiment Data Record (EDR) and Reduced Data Record (RDR) Data Products Archive Bundle. PDS Atmospheres Node. https://doi.org/10.17189/1522849
- Climate predictions using the Mars Climate Database v5.3 (MCD, *e.g.* Forget et al. (1999); Millour et al., 2018)) are accessible at http://www-mars.lmd.jussieu.fr/mcd_python/

References

Papers submitted or in preparation for the same special issue:

- Lemmon M. et al., (accepted, 2022), Dust, Sand, and Winds within an Active Martian Storm in Jezero Crater. *Geophysical Research Letters*; this issue.
- Martínez G. et al., (in prep) Thermal Inertia, Albedo and Surface Energy Budget at Jezero Crater, Mars, as observed from the Mars 2020 MEDA instrument. *Journal of Geophysical Research: Planets*; this issue.
- Munguira A. et al., (submitted), Mars 2020 MEDA Measurements of Near Surface Atmospheric Temperatures at Jezero. *Journal of Geophysical Research*; this issue.
- Pla-Garcia J. et al., (submitted), Nocturnal turbulence at Jezero driven by the onset of a low-level jet as determined from MRAMS and MEDA. *Journal of Geophysical Research*; this issue.
- Stott A. et al., (submitted), The Sensitivity of the SuperCam Microphone to the Martian Atmosphere. *Journal of Geophysical Research*; this issue.
- Sun V. et al., (in prep), Exploring the Jezero Crater Floor: Overview of Results from the Mars 2020 Perseverance Rover's First Science Campaign. *Journal of Geophysical Research*; this issue.
- de la Torre M. et al., (submitted), Diurnal cycle of air temperature fluctuations at Jezero crater. *Journal of Geophysical Research*; this issue.
- Viúdez-Moreira D. et al., (submitted) The near-surface wind patterns as observed by NASA's Mars 2020 Mission at Jezero Crater, Mars. *Journal of Geophysical Research*; this issue.

Mars 2020 papers not published yet:

- Rodríguez Manfredi J.A. et al., (submitted, 2022), The rich meteorology of Jezero crater over the first 250 sols of Perseverance on Mars. *Nature Geoscience*. Doi: https://doi.org/10.21203/rs.3.rs-1634885/v1

Banfield, D., Schindel, D. W., Tarr, S., & Dissly, R. W. (2016). A martian acoustic anemometer. *The Journal of the Acoustical Society of America*, 140(2), 1420-1428. doi: 10.1121/1.4960737

Banfield, D., Rodriguez-Manfredi, J. A., Russell, C. T., Rowe, K. M., Leneman, D., Lai, H. R., … Banerdt, W. B. (2018). InSight auxiliary payload sensor suite (APSS). *Space Science Reviews*, 215(1). doi: 10.1007/s11214-018-0570-x

Banfield, D., Spiga, A., Newman, C., Forget, F., Lemmon, M., Lorenz, R., . . . Banerdt W. B. (2020). The atmosphere of Mars as observed by InSight. *Nature Geoscience*, 13(3), 190-198. doi: 10.1038/s41561-020-0534-0

Bury, Y., Chide, B., Murdoch, N., Cadu, A., Mimoun, D., & Maurice., S. (2019). Wake-induced pressure fluctuations on the Mars2020/SuperCam microphone inform on Martian wind properties. *In EPSC-DPS Joint Meeting* (p. 1589)

Chatain, A., Spiga, A., Banfield, D., Forget, F., & Murdoch, N. (2021). Seasonal variability of the daytime and nighttime atmospheric turbulence experienced by InSight on Mars. *Geophysical Research Letters*, 48(22). doi: 10.1029/2021gl095453

Chide, B., Maurice, S., Murdoch, N., Lasue, J., Bousquet, B., Jacob, X., . . . Wiens R. C. (2019). Listening to laser sparks: a link between laser-induced breakdown spectroscopy, acoustic measurements and

crater morphology. *Spectrochimica Acta Part B: Atomic Spectroscopy*, 153, 50-60. doi: 10.1016/j.sab.2019.01.008

Chide, B., Maurice, S., Cousin, A., Bousquet, B., Mimoun, D., Beyssac, O., . . . Wiens R. C. (2020). Recording laser-induced sparks on mars with the SuperCam microphone. *Spectrochimica Acta Part B: Atomic Spectroscopy*, 174, 106000. doi: 10.1016/j.sab.2020.106000

Chide, B., Beyssac, O., Gauthier, M., Benzerara, K., Estève, I., Boulliard, J.-C., … Wiens R.C. (2021) Acoustic monitoring of laser-induced phase transitions in minerals: implication for mars exploration with SuperCam. *Scientific Reports*, 11(1). doi: 10.1038/s41598-021-03315-7

Christensen, P. R., Mehall, G. L., Silverman, S. H., Anwar, S., Cannon, G., Gorelick, N., … Squyres, S. (2003). Miniature thermal emission spectrometer for the Mars exploration rovers. *Journal of Geophysical Research: Planets*, 108(E12). doi: 10.1029/2003je002117

Davy, R., Davis, J. A., Taylor, P. A., Lange, C. F., Weng, W., Whiteway, J., & Gunnlaugson, H. P. (2010). Initial analysis of air temperature and related data from the phoenix MET station and their use in estimating turbulent heat fluxes. *Journal of Geophysical Research*, 115. doi: 10.1029/2009je003444

Forget, F., Hourdin, F., Fournier, R., Hourdin, C., Talagrand, O., Collins, M., … Huot, J.-P. (1999). Improved general circulation models of the martian atmosphere from the surface to above 80 km. *Journal of Geophysical Research: Planets*, 104(E10), 24155-24175. doi: 10.1029/1999je001025

Gomez-Elvira, J., Armiens, C., Castañer, L., Dominguez, M., Genzer, M., Gomez, F., … Martin Torres, J. (2012). REMS: The environmental sensor suite for the mars science laboratory rover. *Space Science Reviews*, 170(1-4), 583-640. doi: 10.1007/s11214-012-9921-1

Hess, S. L., Henry, R. M., Leovy, C. B., Ryan, J. A., & Tillman, J. E. (1977). Meteorological results from the surface of mars: Viking 1 and 2. *Journal of Geophysical Research*, 82(28), 4559-4574. doi: 10.1029/js082i028p04559

Kaimal, J. C., & Gaynor, J. E. (1991). Another look at sonic thermometry. *Boundary-Layer Meteorology* , 56(4), 401-410. doi: 10.1007/bf00119215

Martinez, G. M., Newman, C. N., Vicente-Retortillo, A. D., Fischer, E., Renno, N. O., Richardson, M. I., … Vasavada, A. R. (2017). The modern near-surface martian climate: A review of in-situ meteorological data from viking to curiosity. *Space Science Reviews*, 212(1-2), 295-338. doi: 10.1007/s11214-017-0360-x

Mason, E. L., & Smith, M. D. (2021). Temperature fluctuations and boundary layer turbulence as seen by mars exploration rovers miniature thermal emission spectrometer *Icarus*, 360, 114350. doi: 10.1016/j.icarus.2021.114350

Maurice, S., Wiens, R. C., Bernardi, P., Cais, P., Robinson, S., Nelson, T., . . . Wong, K. W. (2021). The SuperCam instrument suite on the mars 2020 rover: Science objectives and mast-unit description. *Space Science Reviews*, 217(3). doi: 10.1007/s11214-021-00807-w

Maurice, S., Chide, B., Murdoch, N., Lorenz, R. D., Mimoun, D., Wiens, R. C., . . . and, Willis, P. (2022). In situ recording of mars soundscape. *Nature*, 605(7911), 653-658. doi: 10.1038/s41586-022-04679-0

Millour, E., Forget, F., Spiga, A., Vals, M., Zakharov, V., Montabone, L., … Cipriani, F. (2018). The Mars Climate Database Version 5.3. *In Scientific Workshop: From Mars Express to ExoMars*. ESAC Madrid, Spain https://ui.adsabs.harvard.edu/link_gateway/2018fmee.confE..68M/PUB_PDF

Newman, C. E., Hueso, R., Lemmon, M. T., Munguira, A., Vicente-Retortillo, A., Apestigue, V., … Guzewich, S. D. (2022). The dynamic atmospheric and aeolian environment of jezero crater, mars. *Science Advances*, 8(21). doi: 10.1126/sciadv.abn3783

Petrosyan, A., Galperin, B., Larsen, S. E., Lewis, S. R., Määttänen, A., Read, P. L., … Vazquez, L. (2011). The Martian Atmospheric Bounday Layer. *Reviews of Geophysics*, 49(3). doi: 10.1029/2010rg000351

Rafkin, S., & Banfield, D. (2020). On the problem of a variable mars atmospheric composition in the determination of temperature and density from the adiabatic speed of sound. *Planetary and Space Science*, 193, 105064. doi: 10.1016/j.pss.2020.105064

Read, P. L., Galperin, B., Larsen, S. E., Lewis, S. R., Määttänen, A., Petrosyan, A., … Vazquez, L. (2016). The martian planetary boundary layer. *In R. M. Haberle, R. T. Clancy, F. Forget, M. D. Smith, & R. W. Zurek (Eds.), The atmosphere and climate of mars* (pp. 172-202). Cambridge University Press. doi: 10.1017/9781139060172.007

Rodriguez-Manfredi, J. A., de la Torre Juarez, M., Alonso, A., Apestigue, V., Arruego, I., Atienza, T., … Zurita, S. (2021). The mars environmental dynamics analyzer, MEDA. a suite of environmental sensors for the mars 2020 mission. *Space Science Reviews*, 217(3). doi: 10.1007/s11214-021-00816-9

Schofield, J. T., Barnes, J. R., Crisp, D., Haberle, R. M., Larsen, S., Magalhaaes, J. A., … Wilson, G. (1997). The mars pathfinder atmospheric structure investigation meteorology (ASI/MET) experiment. *Science*, 278(5344), 1752-1758. doi: 10.1126/science.278.5344.1752

Smith, M. D., Wolff, M. J., Lemmon, M. T., Spanovich, N., Banfield, D., Budney, C. J., … Squyres, S. W. (2004). First atmospheric science results from the mars exploration rovers mini-TES. *Science*, 306(5702), 1750-1753. doi: 10.1126/science.1104257

Smith, M. D., Wolff, M. J., Spanovich, N., Ghosh, A., Banfield, D., Christensen, P. R., … Squyres, S. W. (2006). One martian year of atmospheric observations using MER mini-TES. *Journal of Geophysical Research: Planets*, 111(E12). doi: 10.1029/2006je002770

Spanovich, N., Smith, M., Smith, P., Wolff, M., Christensen, P., & Squyres, S. (2006). Surface and near-surface atmospheric temperatures for the mars exploration rover landing sites. *Icarus*, 180(2), 314-320. doi: 10.1016/j.icarus.2005.09.014

Spiga, A. (2019). The planetary boundary layer of mars. *Oxford Research Encyclopedia of Planetary Science*. doi: 10.1093/acrefore/9780190647926.013.130

Wu, Z., Richardson, M. I., Zhang, X., Cui, J., Heavens, N. G., Lee, C., … Witek, M. (2021). Large eddy simulations of the dusty martian convective boundary layer with MarsWRF. *Journal of Geophysical Research: Planets*, 126(9). doi: 10.1029/2020je006752

Rodríguez Manfredi J.A., de la Torre Juarez M., Sanchez-Lavega A., Hueso R., Martinez G., Lemmon M., … Zurita S. et al., (2022), The rich meteorology of Jezero crater over the first 250 sols of Perseverance on Mars. Nature Geoscience. Doi: https://doi.org/10.21203/rs.3.rs-1634885/v1